

A Primer for Manifestly Gauge Invariant Computations in $SU(N)$ Yang-Mills

Oliver J. Rosten

School of Physics and Astronomy, University of Southampton,
Highfield, Southampton SO17 1BJ, U.K.

email: O.J.Rosten@soton.ac.uk

Abstract

It has recently been determined that, within the framework of the Exact Renormalisation Group, continuum computations can be performed to any loop order in $SU(N)$ Yang-Mills theory without fixing the gauge or specifying the details of the regularisation scheme. In this paper, we summarise and refine the powerful diagrammatic techniques which facilitate this procedure and illustrate their application in the context of a calculation of the two-loop β function.

Contents

1	Introduction and Conclusions	2
2	Elements of $SU(N N)$ Gauge Theory	5
3	Diagrammatics	6
3.1	The Exact Flow Equation	6
3.2	Ward Identities	8
3.2.1	Application to Isolated Vertices	8
3.2.2	Application to Complete Diagrams	10
3.3	Taylor Expansion of Vertices	11
3.4	Charge Conjugation Invariance	12
3.5	Perturbative Diagrammatics	14
3.5.1	The Weak Coupling Flow Equations	14
3.5.2	The Effective Propagator Relation	15
3.5.3	Further Diagrammatic Identities	16
4	Universality	17
5	Illustration	17

1 Introduction and Conclusions

The Exact Renormalisation Group (ERG) has, for some time now, provided a framework allowing continuum computations in $SU(N)$ Yang-Mills theory to be performed, without fixing the gauge. Though the earliest formulation [1,2] was constructed in the large N -limit, its subsequent refinement [3] facilitated the first manifestly gauge invariant calculation of the one-loop β -function, β_1 , at finite N . The implementation of a real, gauge invariant cutoff, Λ , was achieved by embedding the physical $SU(N)$ theory in a spontaneously broken $SU(N|N)$ supergauge theory [4]. Guided by the universality of the answer, the calculation of β_1 was performed without specifying the precise details of the regularisation scheme, leading to a partially diagrammatic computational methodology.

Besides the coupling, $g(\Lambda)$, of the physical $SU(N)$ gauge field, A^1 , there is a second coupling, $g_2(\Lambda)$, associated with an unphysical $SU(N)$ field, A^2 , that requires separate renormalisation [5{7].¹ (This unphysical field is part

¹For technical reasons, a superscalar field is given zero mass dimension [3], and thus is associated by the usual dimensional reasoning with an infinite number of dimensionless couplings. These couplings do not require renormalisation [6,8].

of the $SU(N_f N_c)$ regularising structure.) Respecting this fact, whilst preserving the powerful diagrammatic techniques of [3] beyond one loop, required generalisation of the formalism. This challenging problem, finally overcome in [6,7], yielded the first manifestly gauge invariant, continuum calculation of the two-loop function [6,8], Γ_2 . The practical execution of this calculation necessitated the major development of the original diagrammatic techniques, not only for calculational convenience, but also to elucidate the structure of the new ERG (or flow) equation [6{8].

The considerable amount of detail present in [6{8] reflects the subtlety and complexity of the new flow equation. However, the actual rules for performing perturbative calculations (of function coefficients, at any rate; generalisation of the methods is planned for the future [9]) are remarkably simple, as a consequence of the diagrammatics. In this paper, we summarise the primary diagrammatic rules and use the illustration of their application to significantly refine the calculational procedure of [7] (see also [6]).

Contrary to previous works [3,5{7], the flow equation is introduced via its diagrammatic representation and thus is never explicitly written down. Hence, we do not work with a single flow equation but rather with an infinite class which obey the same diagrammatic rules. (It is assumed that the general properties which all good flow equations possess [3,5,10{12] e.g. invariance of physics under the flow and etc. are implicitly satisfied.)

Within our ERG, the flow is controlled by a (generically) non-universal object, \hat{S} , the ‘seed action’ [3,6{8,11{13]. This respects the same symmetries as the Wilsonian effective action, S , and has the same structure. However, whereas our aim is to solve the flow for S , \hat{S} acts as an input. In accord with our general philosophy, the seed action is left unspecified where possible and implicitly defined where necessary. There is one important exception to this, at the heart of the diagrammatic techniques: it is technically useful to set the two-point, tree level seed action vertices equal to their Wilsonian effective action counterparts. In turn, this ensures that, if the flow equation is sufficiently general [7], then for each two-point, tree level vertex (that cannot be consistently set to zero) there exists an ‘effective propagator’, which plays a crucial diagrammatic rôle. These effective propagators, denoted by Δ , are the inverses of the two-point, tree level vertices up to remainder terms [3] (in the gauge sector); we call this the ‘effective propagator relation’ [3]. The remainder terms appear as a consequence of the manifest gauge invariance: the effective propagators are inverses of the two-point, tree level vertices only in the transverse space. It is important to emphasise that the effective propagators are by no means propagators in the usual sense, but their name recognises their similarity in both form and diagrammatic function.

In this paper we will sketch how, starting from a diagrammatic expression for Γ_2 involving the seed action action and details of the covariantisation of the

cuto, we can derive an expression with no explicit dependence on these non-universal objects. The basic strategy is to recognise that amongst the terms generated by the flow equation are manipulable diagrams comprising exclusively Wilsonian effective action vertices joined together by ϕ -where, having defined

$$\frac{g_2^2}{g^2}; \quad (1)$$

we define

$$X = \partial_j X; \quad (2)$$

∂_j being the generator of the ERG flow. The manipulable diagrams are processed by moving ∂_j from the effective propagator to strike the diagram as a whole, minus correction terms in which ∂_j strikes the vertices. The former terms, called ∂ -derivative terms, are those from which the numerical value of β_2 can be directly extracted [6,8]; the latter terms can be processed using the flow equation and the resulting set of diagrams simplified, using primary diagrammatic identities. At this point, we are able to identify cancellations of non-universal contributions.

Iterating this procedure, the diagrammatic expression can be reduced exclusively to ∂ -derivative terms and ϕ -term s', though we note that there is a complication to this diagrammatic procedure: particular sub-diagrams can have two distinct diagrammatic representations. The equivalence of these representations is encoded in the secondary diagrammatic identities, of which a sub-set are presented here. For the complete set, the reader is referred to [6]. The ϕ -terms are an artifact of the $SU(N_f)$ regularisation scheme and vanish, as they must, in the limit that $\epsilon \rightarrow 0$ [6,8].

Compared with [7], we realise that, at each stage of the calculation, both the cancellation of non-universal contributions and the creation of ∂ -derivative terms can each be done in parallel. This vastly simplifies the calculational procedure, the benefits becoming increasingly pronounced with each loop order. Despite this important development, even at two-loops a β function calculation still has many steps. However, the illustration of the β_2 diagrammatics will serve to demonstrate that the procedure is algorithmic. As we will see in [14] (see also [6] for an incomplete discussion), this can be turned very much to our advantage: using the techniques of this paper, we can jump straight from the initial expression for a β function coefficient to the ∂ -derivative and ϕ -term s, to all orders in perturbation theory. At a stroke, this removes the major difficulty associated with performing computations within our framework, leaving open the exciting prospect of a manageable, manifestly gauge invariant calculus for $SU(N_f)$ Yang-Mills theory.

Section 2 introduces the necessary elements of $SU(N_f)$ gauge theory, for our purposes. In section 3 we describe the diagrammatics. First, we give the

diagrammatic representation of the exact flow equation. Secondly, we describe the diagrammatic realisation of the Ward identities. Thirdly, we show how the various vertices of the objects involved in the flow equation can be Taylor expanded. Lastly, we specialise the diagrammatics to the perturbative domain. In section 5, we illustrate the use of the diagrammatics in the context of a computation of the perturbative two-loop function.

2 Elements of $SU(N|N)$ Gauge Theory

Denoting the supergauge field, by A which transforms under the adjoint of $SU(N|N)$ we embed the physical field A^1 in a supertraceless, Hermitian supermatrix as follows:

$$A = \begin{pmatrix} A^1 & B \\ B & A^2 \end{pmatrix} + A^0 \mathbb{1};$$

where A^2 carries an unphysical $SU(N)$ gauge theory, B and B are wron statistics gauge fields and $A^0 \mathbb{1}$ is a central term.

The theory is locally invariant under:

$$A = [r; (x)] + \mathbb{1}; \quad (3)$$

The first term, in which $r = \partial_\mu + iA_\mu$, generates supergauge transformations. Note that the coupling, g , has been scaled out of this definition. It is worth doing this: since we do not gauge x , the exact preservation of (3) means that none of the fields suffer field strength renormalisation, even in the broken phase [3].

The second term in (3) divides out the centre of the algebra. This ‘ A^0 shift symmetry’ ensures that nothing depends on A^0 and that A^0 has no degrees of freedom. We adopt a prescription whereby we can effectively ignore the field A^0 , altogether, using it to map us into a particular diagrammatic picture [6, 7].

For the superscalar field, C , which spontaneously breaks the $SU(N|N)$ invariance, there is no need to factor out the central term [4] and so we write

$$C = \begin{pmatrix} C^1 & D \\ D & C^2 \end{pmatrix};$$

This field transforms covariantly:

$$C = i[C; \cdot];$$

In order that, at the classical level, the spontaneous breaking scale tracks the covariant higher derivative effective cutoff scale, Λ , we take C to be dimensionless and demand that \hat{S} has the minimum of its effective potential at

$$\langle C \rangle = \begin{pmatrix} 11 & 0 \\ 0 & 11 \end{pmatrix} : \quad (4)$$

In this case the classical action S_0 also has a minimum at (4). Ensuring that this is not destroyed by quantum corrections demands that the Wilsonian effective action one-point C^1 , C^2 vertices vanish [3, 6, 7], which can be translated into a constraint on \hat{S} .

Working in the broken phase, the fermionic fields $B; \bar{B}$ and $D; \bar{D}$ can be combined into composite fields, $F_M = (B; \bar{D})$, $F_N = (\bar{B}; D)$, where M, N are vector indices [6, 8].² This simplification recognises that, via the Higgs mechanism, B and D gauge transform into each other and so propagate as a composite object.

In $SU(N|N)$ gauge theory, the supertrace replaces the trace as the natural cyclic invariant [4, 15]. The manifestly gauge invariant Wilsonian effective action, S , comprises supertraces and products of supertraces where the arguments of the supertraces are sets of net-bosonic fields.

3 Diagrammatics

In recognition of the central rôle played by the diagrammatics, our approach is generally to first state the diagrammatic rules and then to describe the various elements involved.

3.1 The Exact Flow Equation

The ERG equation can be represented as shown in figure 1 [6, 7].

$$\textcircled{\bullet} \textcircled{S} \stackrel{\text{ffg}}{=} \frac{1}{2} \textcircled{g} \textcircled{S} + \textcircled{g} + \textcircled{g} \textcircled{} + \textcircled{g} \textcircled{} \textcircled{} + 3 \textcircled{g} \textcircled{} \textcircled{}$$

Figure 1: The diagrammatic form of the flow equation.

²The summation convention for these indices is that we take each product of components to contribute with unit weight.

The left-hand side depicts the flow of all independent Wilsonian effective action vertex coefficient functions, which correspond to the set of fields, ffg. Each coefficient function has associated with it an implied supertrace structure (and symmetry factor which, as one would want, does not appear in the diagrammatics). For example,

$$\begin{array}{c} \text{C}^1\text{C}^1 \\ \textcircled{\text{S}} \end{array}$$

represents both the coefficient functions $S^{\text{C}^1\text{C}^1}$ and $S^{\text{C}^1\text{C}^1}$ which, respectively, are associated with the supertrace structures strC^1C^1 and $\text{strC}^1\text{strC}^1$.

The objects on the right-hand side of figure 1 have two different types of component. The lobes represent vertices of action functionals, where $g^2 S = 2\hat{S}$. The object attaching to the various lobes, --- , is the sum over vertices of the covariantised ERG kernels [1, 3] and, like the action vertices, can be decorated by fields belonging to ffg. The fields of the action vertex (vertices) to which the vertices of the kernels attach act as labels for the ERG kernels though, in certain circumstances, the particular decorations of the kernel are required for unambiguous identification [6, 7]. However, in actual calculations, these non-universal details are irrelevant. We loosely refer to both individual and summed over vertices of the kernels simply as a kernel. Note that kernels labelled at one end by either A or B and at the other by either C or D do not exist [3].

The nald diagram on the right-hand side contains a kernel which bites its own tail. Such diagrams are not properly UV regulated and, in the past, it has been argued that they can and should be discarded [1, 3, 7, 16]. Here, we will keep these diagrams: as recognised in [6], in any calculation of universal quantities, the ultraviolet divergences in kernel-biting-their-tail diagrams are cancelled by implicit divergences in other terms, such diagrams always disappearing in the final answer [6, 9, 14]. We will see an explicit example of this in section 5.

The rule for decorating the complete diagrams on the right-hand side is simple: the set of fields, ffg, are distributed in all independent ways between the component objects of each diagram.

Embedded within the diagrammatic rules is a prescription for evaluating the group theory factors. Suppose that we wish to focus on the flow of a particular vertex coefficient function, which necessarily has a unique supertrace structure. On the left-hand side of the flow equation, we can imagine splitting the lobe up into a number of lobes equal to the number of supertraces (traditionally, these lobes would be joined by dotted lines, to indicate that they are part of the same vertex [6, 7]). To finish the specification of the vertex coefficient function, the lobes should be explicitly decorated by the fields ffg, where the fields are, in this picture, to be read off each lobe in the counterclockwise sense.

On the right-hand side of the flow equation, things are slightly more complicated. Each lobe is, in principle a multi-supertrace object, and the kernel can attach to any of these supertraces. The kernel itself is a multi-supertrace object [for more details see [6,7]] but, for our purposes, we need note only that the kernel is, in this more explicit diagrammatic picture, a double sided object. Thus, whilst the dumbbell like term of figure 1 has at least one associated supertrace, the next two diagrams have at least two, on account of the loop. If a closed circuit formed by a kernel is devoid of fields then it contributes a factor of N , depending on the flavours of the fields to which the kernel forming the loop attaches. This is most easily appreciated by defining the projectors

$$+ \begin{array}{cc} & ! \\ 11 & 0 \\ 0 & 0 \end{array} ; \quad \begin{array}{cc} & ! \\ 0 & 0 \\ 0 & 11 \end{array}$$

and noting that $\text{str} = N$. In the counterclockwise sense, a $+$ can always be inserted after an A^1, C^1 or F , whereas a $-$ can always be inserted after an A^2, C^2 or F .

The rules thus described receive $1=N$ corrections in the A^1 and A^2 sectors. If a kernel attaches to an A^1 or A^2 , it comprises a direct attachment and an indirect attachment, as shown in figure 2.

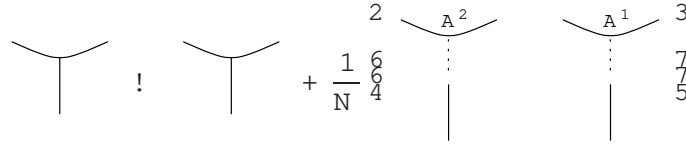


Figure 2: The $1=N$ corrections to the group theory factors.

We can thus consider the diagram on the left-hand side as having been unpackaged, to give the terms on the right-hand side (note that, in this context, the first diagram on the right-hand side cannot itself be unpackaged; here, the attachment is just the direct one). The dotted lines in the diagrams with indirect attachments serve to remind us where the loose end of the kernel attaches in the parent diagram.

3.2 Ward Identities

3.2.1 Application to Isolated Vertices

All vertices, whether they belong to either of the actions or to the covariantised kernels are subject to Ward identities. Due to the manifest gauge invariance,

these take a particularly simple form, as shown in figure 3. This is our first example of a primary diagrammatic identity.

Figure 3: The Ward identities.

On the left-hand side, we contract a vertex with the momentum of the field which carries p . This field which we will call the active field can be either A^1 , A^2 , F_R or F_R . In the first two cases, the open triangle represents p whereas, in the latter two cases, it represents $p_R = (p; 2)$ [6, 7]. (Given that we often sum over all possible fields, we can take the Feynman rule for in the C -sector to be null.)

On the right-hand side, we push the contracted momentum forward onto the field which directly follows the active field, in the counterclockwise sense, and pull back (with a minus sign) onto the field which directly precedes the active field. Since our diagrammatics is permutation symmetric, the struck field which we will call the target field can be either X , Y or any of the un-drawn fields represented by the ellipsis. Any field(s) besides the active field and the target field will be called spectators. Note that we can take X and $/$ or Y to represent the end of a kernel. In this case, the struck field is determined to be unambiguously on one side of the (double sided) kernel; the contributions in which the struck field is on the other side are included in the ellipsis. This highlights the point that allowing the active field to strike another field necessarily involves a partial specification of the supertrace structure: it must be the case that the struck field either directly followed or preceded the active field. In turn, this means that the Feynman rule for particular choices of the active and target fields can be zero. For example, an F can follow, but never precede an A^1 , and so the pullback of an A^1 onto an F should be assigned a value of zero. The momentum routing follows in obvious manner: for example, in the first diagram on the right-hand side, momentum $q + p$ now flows into the vertex. In the case that the active field is fermionic, the field pushed forward / pulled back onto is transformed into its opposite statistic partner. There are some signs associated with this in the C and D -sectors, which we will not require here [6, 7]; for calculations of universal quantities, they are hidden by the diagrammatics.

The half arrow which terminates the pushed forward / pulled back active field is of no significance and can go on either side of the active field line. It

is necessary to keep the active eld line| even though the active eld is no longer part of the vertex| in order that we can unambiguously deduce flavour changes and momentum routing, without reference to the parent diagram.

3.2.2 Application to Complete Diagrams

Consider the flow of a (Wilsonian effective action) vertex which is contracted with the momentum of one of its elds. Suppose that, in addition to the active eld, the vertex is decorated by the set of elds ff^0g . Referring back to figure 1, the left-hand side becomes the sum of vertices decorated by ff^0g where, for each diagram in the sum, one of the elements of ff^0g is either pushed forward or pulled back onto by the active eld.

The right-hand side of figure 1 now comprises three different types of diagram. The active eld can either push forward or pull back

1. onto one of the elements of ff^0g ;
2. round an action vertex onto an internal eld;
3. onto the end of a kernel.

An example of a diagram of either the second or third type is shown in figure 4.

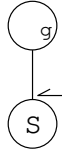


Figure 4: Example of a diagram in which the active eld strikes an internal eld.

Recalling that, if the active eld is fermionic, the flavour of the struck eld will change, attachment corrections of the type shown in figure 2 must be worked out after the action of the active eld, and according to whether the eld attached to (rather than the eld at the end of the kernel, which will be of a different flavour) is in the $A^{1/2}$ sector [6].

By gauge invariance, it must be the case that the sum over all diagrams of the second and third types vanishes [7] (see [6] for an explicit demonstration of this). This follows since we are simply computing the flow of a vertex (albeit one in which one of the elds can be thought of as having been struck by a active

eld). From gure 1, we know that there cannot be any surviving contributions in which internal elds are pushed forward / pulled back onto.³

3.3 Taylor Expansion of Vertices

For the formalism to be properly defined, it must be the case that all vertices are Taylor expandable to all orders in momenta [1, 2, 17]. For the purposes of this paper, we need only the diagrammatic rules for a particular scenario. Consider a vertex which is part of a complete diagram, decorated by some set of internal elds and by a single external A^1 (or A^2). The diagrammatic representation for the zeroth order expansion in the momentum of the external eld is all that is required and is shown in gure 5 [6, 7]; note the similarity to gure 3.

Figure 5: Diagrammatic representation of zeroth order Taylor expansion.

The interpretation of the diagrammatics is as follows. In the first diagram on the right-hand side, the vertex is differentiated with respect to the momentum carried by the eld X , whilst holding the momentum of the preceding eld fixed. Of course, using our current diagrammatic notation, this latter eld can be any of those which decorate the vertex, and so we sum over all possibilities. Thus, each cyclically ordered push forward like term has a partner, cyclically ordered pullback like term, such that the pair can be interpreted as

$$\partial_s^r \partial_r^s \text{Vertex}; \quad (5)$$

where r and s are momenta entering the vertex. In the case that $r = s$, we can and will drop either the push forward like term or pullback like term, since the combination can be expressed as ∂_s^r ; we interpret the diagrammatic notation appropriately. Just as in gure 3, the elds X and or Y can be interpreted as the end of a kernel. In this case, we introduce some new notation, since it proves confusing in complete diagrams to actually locate the derivative symbol at the end of such an object. The notation for the derivative with respect to the momentum entering the end of a kernel is introduced in gure 6.

³In function calculations, where active elds arise in a different context, diagrams in which internal elds are pushed forward / pulled back onto can survive.

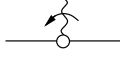


Figure 6: Notation for the derivative with respect to the momentum entering an undecorated kernel.

Recalling that a kernel, whose elds are explicitly cyclically ordered, is a two-sided object, we first note that the eld whose momentum we have expanded in is sat on the top-side of the vertex. The derivative is taken to be with respect to the momentum which flows into the end of the vertex which follows the derivative, in the sense indicated by the arrow on the derivative symbol. It is clear that the direction of the arrow on the derivative symbol can be reversed at the expense of a minus sign.

3.4 Charge Conjugation Invariance

Charge conjugation invariance can be used to simplify the diagrammatics, by allowing us to discard certain terms and to combine others. The diagrammatic rule for replacing a diagram with its charge conjugate is to reflect the diagram, picking up a sign for every external A^1 or A^2 and letting $F \rightarrow F$ [6, 7] (we temporarily assume that no Taylor expansions have been performed and that, should any of the elds be contracted with their momentum, the Ward identities are yet to be applied).

Charge conjugation is of particular use in complete diagrams for which all external elds are bosonic. In this case, charge conjugation effectively never changes eld flavours. The only such changes induced by charge conjugation are in the fermionic sector where, after reflection, we must change $F \rightarrow F$. However, by taking all external elds to be bosonic, these changes now only affect internal elds, whose flavours are summed over anyway.

Thus, for example, a diagram possessing only bosonic external elds (and any number of internal elds) must possess an even number of external $A^{1/2}$ elds but any number of external $C^{1/2}$ elds.

It is straightforward to extend the diagrammatic rule for charge conjugation to include diagrams containing momentum derivatives and / or application of the Ward identities [6, 7]. Supplementing the previous rule, we simply pick up a minus sign for each momentum derivative and for each application of the Ward identities [6, 7]. Note that active elds which have been processed by the Ward identities should still be counted when we sum up the number of external

A^1 s and A^2 s; this is intuitive from a diagrammatic point of view, since the eld line is kept, but now terminates in a half arrow, rather than entering a vertex.

This allows us to simplify the set of terms generated either by an application of the Ward identities or by a Taylor expansion. To illustrate this, we need deal only the former case, due to the similarity of the diagrammatic rules for each. Consider a diagram generated by a single application of the Ward identities, in which no Taylor expansions have been performed. We focus on a single target eld, which we know can be both pushed forward and pulled back onto, as shown in figure 7.

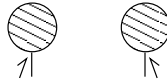


Figure 7: Sum of the push forward and pull back onto the same target eld.

The assumption that the diagram contains no further target elds or momentum derivative tells us that the supertrace structure of all spectator elds is unspecified. That all external elds are bosonic ensures that charge conjugation leaves the eld content of the diagram unchanged. Thus, reflecting either diagram of figure 7, we can combine terms with the other diagram. Whether contributions add or cancel depends on whether the diagrams as a whole are charge conjugation odd or even.

Given that we have combined terms in this way, suppose that there is a second active eld (or that we perform a Taylor expansion). Using the Ward identities, we once again find that each target eld is both pushed forward and pulled back onto. Now, however, such terms cannot be combined, since the supertrace structure of the elds which spectate with respect to this second application of the Ward identities have a partially specified supertrace structure, themselves. Consider the complete set of diagrams generated by any number of applications of the Ward identities and possessing any number of momentum derivatives. For each factorisable sub-diagram, we can combine one push forward with one pull back; thereafter, we cannot combine terms further.

In our example calculation of \mathcal{Z}_2 , we will encounter active elds attached to internal lines. Since the flavour of internal lines is summed over, we can combine pushes forward with pulls back of these elds, using the recipe above.

3.5 Perturbative Diagrammatics

In the perturbative domain, we have the following weak coupling expansions [1, 3, 6, 7]. The Wilsonian effective action is given by

$$S = \sum_{i=0}^{\infty} g^{2i+1} S_i = \frac{1}{g^2} S_0 + S_1 + \dots; \quad (6)$$

where S_0 is the classical effective action and the $S_{i>0}$ the i th-loop corrections. The seed action has a similar expansion:

$$\hat{S} = \sum_{i=0}^{\infty} g^{2i} \hat{S}_i; \quad (7)$$

Recalling (1) we have:

$$\partial g = \sum_{i=1}^{\infty} g^{2i+1} \Gamma_i(\cdot) \quad (8)$$

$$\partial = \sum_{i=1}^{\infty} g^{2i} \Gamma_i(\cdot): \quad (9)$$

3.5.1 The Weak Coupling Flow Equations

Defining $\hat{\Gamma}_i = S_i - 2\hat{S}_i$, the weak coupling flow equations follow from substituting (6)-(9) into the flow equation, as shown in figure 8 [6, 7].

$$\begin{aligned} \text{"} \quad \textcircled{n} \quad \#_{\text{ffg}} &= \sum_{r=0}^{\infty} \frac{1}{2} \sum_{n_r=0}^{\infty} \frac{X^{n_r}}{g^{2n_r+1}} \left(\textcircled{n_r} \right) + \frac{\partial}{\partial g} \left(\textcircled{n_r} \right) \\ &+ \frac{1}{2} \sum_{n_r=0}^{\infty} \frac{X^{n_r}}{g^{2n_r+1}} \left(\textcircled{n_r} \right) + \frac{1}{2} \sum_{n_r=0}^{\infty} \frac{X^{n_r}}{g^{2n_r+1}} \left(\textcircled{n_r} \right) + \frac{1}{2} \sum_{n_r=0}^{\infty} \frac{X^{n_r}}{g^{2n_r+1}} \left(\textcircled{n_r} \right) \end{aligned} \quad (10)$$

Figure 8: The weak coupling flow equations.

We refer to the first two terms on the right-hand side of (10) as Γ and $\partial \Gamma$ terms, respectively. The symbol ∂ , as in equation (2), means $\partial/\partial g$. A vertex whose argument is an undorned letter, say n , represents S_n . We define $n_r = n - r$ and $n = n_r + 1$. The bar notation of the dumbbell term is defined as follows:

$$a_0[S_{n-r}; S_r] = a_0[S_{n-r}; S_r] - a_0[S_{n-r}; \hat{S}_r] - a_0[\hat{S}_{n-r}; S_r]:$$

3.5.2 The Effective Propagator Relation

The effective propagator relation [3] is central to the perturbative diagrammatic approach, and arises from examining the flow of all two-point, tree level vertices. This is done by setting $n = 0$ in (10) and specialising ffg to contain two fields, as shown in figure 9. We note that we can and do choose all such vertices to be single supertrace terms [6, 7].

$$\text{Diagram 1} = \text{Diagram 2} \quad (11)$$

Figure 9: Flow of all possible two-point, tree level vertices.

Following [13, 6, 7, 12, 16], we use the freedom inherent in \hat{S} by choosing the two-point, tree level seed action vertices equal to the corresponding Wilsonian effective action vertices. Equation (11) now simplifies. Rearranging, integrating with respect to ϕ and choosing the appropriate integration constants [6, 7], we arrive at the relationship between the integrated ERG kernels| a.k.a. the effective propagators| and the two-point, tree level vertices shown in figure 10. Note that we have attached the effective propagator, which only ever appears as an internal line, to an arbitrary structure.

$$\text{Diagram 1} + \text{Diagram 2} + \text{Diagram 3} + \text{Diagram 4} + \text{Diagram 5} \quad (12)$$

Figure 10: The effective propagator relation.

We have encountered Δ already, in section 3.2. Of Δ , all we need know for our purposes is that it carries an index, M , which is a four-index in the A^1, A^2 sectors, and a \bar{a} index in the F^1, F^2 sectors. In the C sector, Δ is null [3, 6, 7]. The structure Δ is a 'gauge remainder' [3]. The individual components of Δ will often be loosely referred to as gauge remainders; where it is necessary to unambiguously refer to the composite structure, we will use the terminology 'full gauge remainder'.

It is important to note that we have defined the diagrammatics in figure 10 such that there are no $1/N$ corrections where the effective propagator attaches to the two-point, tree level vertex. We do this because, when the composite object on the left-hand side of figure 10 appears in actual calculations, it always occurs inside some larger diagram. It is straightforward to show that, in this case, the aforementioned attachment corrections always vanish [6].

3.5.3 Further Diagrammatic Identities

We begin with a diagrammatic identity which follows from gauge invariance and the constraint placed on the vertices of the Wilsonian effective action by the requirement that the minimum of the Higgs potential is not shifted by quantum corrections:

$$\text{---} \triangleright \bigcirc(0) \text{---} = 0: \quad (13)$$

This follows directly in the A-sector, since one-point A-vertices do not exist. In the F-sector, though, we are left with one-point C^1 and C^2 -vertices, but these are constrained to be zero.

From the effective propagator relation and (13), two further diagrammatic identities follow. First, consider attaching an effective propagator to the right-hand end in (13) and applying the effective propagator before has acted. Diagrammatically, this gives

$$\triangleright \bigcirc(0) \text{---} = 0 = \triangleright \triangleright \triangleright \triangleright ;$$

which implies the following diagrammatic identity:

$$\triangleright \triangleright = 1: \quad (14)$$

The effective propagator relation, together with (14), implies that

$$\text{---} \bigcirc(0) \longrightarrow = \triangleright \triangleright \triangleright \triangleright = 0:$$

In other words, the (non-zero) structure \longrightarrow kills a two-point, tree level vertex. But, by (13), this suggests that the structure \longrightarrow must be equal, up to some factor, to \triangleleft . Indeed,

$$\longrightarrow \triangleleft \text{---} \text{---} \text{---} ; \quad (15)$$

where dot-dash line represents the pseudo effective propagators of [6, 7].

The final diagrammatic identity we require follows directly from the independence of on :

$$= 0: \quad (16)$$

4 Universality

To compute a universal quantity, we must feed in a physical input, which is done via the renormalisation condition [1, 3]:

$$S[A = A^1; C = C] = \frac{1}{2g^2} \text{tr} \int d^D x F^{12}{}^2 + \dots; \quad (17)$$

where the ellipsis denotes higher dimension operators and ignored vacuum energy and C is the location of the minimum of the Higgs potential. This forces

$$S_0^{11}(p) = 22(p) + O(p^4);$$

where the 1s are shorthand for A^1 s and the $O(p^4)$ contributions to the vertex are non-universal. We can arrange calculations of universal function coefficients and, presumably, of all universal quantities such that the answer is manifestly controlled by the renormalisation condition [6, 8, 13].

When computing α_2 , we must remove all contributions arising from the running of α in order to obtain agreement with the standard, universal answer; this is done by tuning $\alpha \rightarrow 0$ at the end of the calculation [6, 8].⁴ Note that the α_i of (9) are determined by the renormalisation condition for the unphysical coupling, g_2 :

$$S[A = A^2; C = C] = \frac{1}{2g^2} \text{tr} \int d^D x F^{22}{}^2 + \dots;$$

5 Illustration

To illustrate the diagrammatic techniques in action, we will perform the initial stages of a computation of α_2 . To start, we specialise the weak coupling flow equations (10) to $n = 2$, take $\text{ffg} = A^1 A^1$ and work at $O(p^2)$. The renormalisation condition (17) implies that $S_1^{11}(p) = O(p^4)$ and so we are left with an algebraic equation for α_2 , as shown in figure 11. The Lorentz indices of the external elds are suppressed.

Diagrams are labelled in boldface. If a diagram is cancelled, then its reference number is enclosed in curly braces, together with the reference number of the diagram against which it cancels. If the reference number of a diagram is followed by an arrow, the arrow points to the figure where the diagram is processed. Since we are not performing the complete diagrammatics for α_2 ,

⁴Of course, disagreement with the standard value of α_2 is not necessarily a signature of a sick formalism, since α_2 is not physically observable and is only expected to agree between two differing schemes under certain conditions.

$$4 \text{ } 2 \text{ } 2 \text{ } (p) + O(p^4) = \frac{1}{2} \left(\text{Diagram D.1} \right) + \text{Diagram D.2} + \text{Diagram D.3}$$

Diagram D.1: A circle with a vertical line of 6 loops on the left and a horizontal line of 2 loops on the top. The circle is labeled '1'.

Diagram D.2: A circle with a vertical line of 2 loops on the left and a horizontal line of 2 loops on the top. The circle is labeled '1'.

Diagram D.3: A circle with a vertical line of 7 loops on the left and a horizontal line of 2 loops on the top. The circle is labeled '2r' and 'r'.

Figure 11: Diagrammatic equation for ϕ^2 .

not all diagrams are labelled and, of those that are, not all are processed or cancelled.

When explicitly decorating with the external fields, we note that they are identical, by Bose symmetry. Thus, for terms in which the two fields decorate separate structures, we can simply draw a single diagram but pick up a factor of two.

For each diagram generated by the flow, our strategy is as follows. First, we isolate the component for which all vertices are Wilsonian effective action vertices and for which the kernel is undecorated, should it exist. To facilitate this separation, we introduce the symbol undecorated to indicate an undecorated kernel and decorated such that, when operating on a kernel, $\text{decorated} = \text{undecorated} + \text{decorated}$. In certain circumstances, we will be able to trade symbols; for example, if a kernel carries undecorated but possesses an explicit decoration, then we can replace decorated by undecorated . The manipulable component of diagram D.1 is isolated in figure 12.

$$\frac{1}{2} \left(\text{Diagram D.4} \right) = \frac{1}{2} \left(\text{Diagram D.5} \right) + \text{Diagram D.6}$$

Diagram D.4: A circle with a vertical line of 6 loops on the left and a horizontal line of 2 loops on the top. The circle is labeled '1'.

Diagram D.5: A circle with a vertical line of 6 loops on the left and a horizontal line of 2 loops on the top. The circle is labeled '1'.

Diagram D.6: A circle with a vertical line of 7 loops on the left and a horizontal line of 2 loops on the top. The circle is labeled '1'.

Figure 12: Isolating the manipulable component for diagram D.1.

Notice that this diagrammatic step has been performed without explicitly decorating terms with the external fields, thereby reducing the number of terms we have to deal with. This is the first refinement of the computational methodology employed in [7].

Next, there follows a two-step process. First, we convert diagram D.4 into a ϕ -derivative term, by moving the ϕ -derivative off the effective propagator. This is shown in the first line of figure 13. On the second line, we promote

the effective propagator to an implicit decoration; this promotion is the second refinement of the diagrammatics.

$$\frac{1}{2} \begin{array}{c} 2 \\ \circlearrowleft \\ 4 \end{array} \begin{array}{c} 3_{11} \\ \circlearrowright \\ 5 \end{array} = \frac{1}{2} \begin{array}{c} 2'' \\ \circlearrowleft \\ 4 \end{array} \# \begin{array}{c} 3_{11} \\ \circlearrowright \\ 5 \end{array} = \frac{1}{2} \begin{array}{c} 2 \\ \text{D.7} \\ \frac{6}{4} \end{array} \begin{array}{c} 1 \\ \circlearrowleft \\ 4 \end{array} + \frac{1}{2} \begin{array}{c} 2 \\ \text{D.8 ! 14} \\ \frac{8}{4} \end{array} \begin{array}{c} 3_{11} \\ \circlearrowright \\ 5 \end{array}$$

Figure 13: Converting diagram D.4 into a ∂ -derivative term.

Notice that we have replaced ∂ by ∂'' , since we take these symbols to mean the same thing, i.e. just ∂_j , when operating on a vertex or effective propagator.

Diagram D.7 is a ∂ -derivative term. The vertex is enclosed in square brackets which tells us that ∂_j is taken to act after explicit decoration. However, in diagram D.8, it is just the vertex which is struck by ∂_j ; this term is processed using the flow equation, as shown in figure 14.

$$\frac{1}{2} \begin{array}{c} 11 \\ \circlearrowleft \\ 1 \end{array} = \begin{array}{c} 2 \\ \text{D.9 ! 15} \\ \frac{6}{4} \end{array} \begin{array}{c} 1_r \\ \circlearrowleft \\ r \end{array} + \begin{array}{c} 2 \\ \text{D.10} \\ \frac{6}{4} \end{array} \begin{array}{c} 1 \\ \circlearrowleft \\ 0 \end{array} + \begin{array}{c} 3_{11} \\ \text{D.11} \\ \frac{7}{5} \end{array} \begin{array}{c} 1 \\ \circlearrowleft \\ 0 \end{array}$$

Figure 14: Result of processing diagram D.8 with the one-loop flow equation.

There now follows a crucial step in the diagrammatic procedure: we recognise that diagram D.9 possesses two-point, tree level vertices that can be attached to either the external fields or the effective propagator. In the former

case, this generates a structure which is manifestly $O(p^2)$, allowing us to Taylor expand at least some of the diagram's other structures in p . In the latter case, we can apply the effective propagator relation.

To facilitate the separation of the two-point, tree level vertices, we define the reduced, n -loop vertex thus:

$$V_n^R = \begin{cases} V_n & n > 0 \\ v_{0RS}^{XX}(k) & n = 0 \end{cases};$$

where we have suppressed all arguments of the generic vertex, v_n , and its reduction. By definition, the reduced vertex does not contain a two-point, tree level component. A superscript number in a vertex argument denotes the total number of fields which must decorate the given vertex e.g. 0^2 is the argument of a two-point, tree level vertex. Using this notation, we isolate the two-point, tree level vertices of diagram D.9 in figure 15.

Figure 15: Isolation of the two-point, tree level vertices of diagram D.9.

Diagram D.12 simplifies. First, we note that $1^R = 1$, by definition. Secondly, we note that

$$a_0[S_n; S_0^2] = a_0[S_n; S_0^2] = a_0[S_n; \hat{S}_0^2] = a_0[\hat{S}_n; S_0^2] = a_0[\hat{S}_n; \hat{S}_0^2]; \quad (18)$$

where the last step follows from the equality of the Wilsonian effective action and seed action two-point, tree level vertices. Performing this simplification, we decorate the two-point, tree level vertex, to give the diagrams of figure 16.

The relative factor of two in diagrams D.13 and D.14 comes from having been able to attach the effective propagator either way round. Explicit decoration with an external A^1 is denoted by a wiggly line, as exemplified in diagram D.15. Were we to decorate this diagram with the remaining external field, we would pick up a factor of two, since the external fields would appear on different structures.

Diagrams D.13 and D.14 can be processed using the effective propagator relation (12), to give the terms of figure 17.

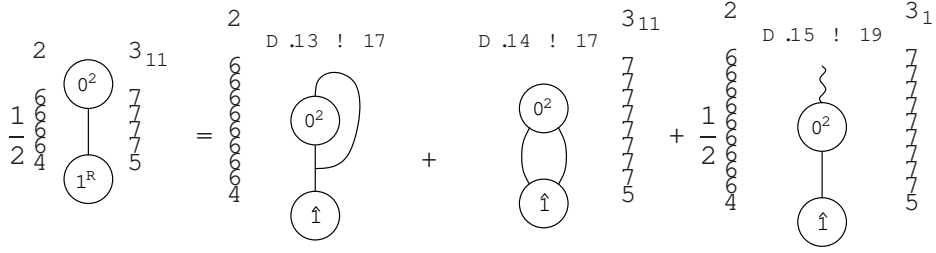


Figure 16: Decorating the two-point, tree level vertex of diagram D.12.

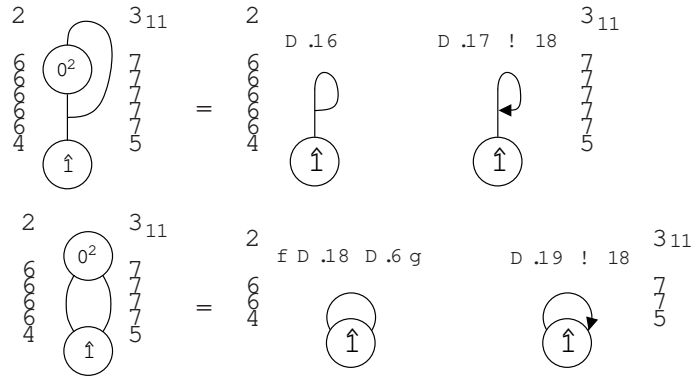


Figure 17: Processing diagrams D.13 and D.14 with the effective propagator relation.

The structure of the calculation now begins to reveal itself, as we find two cancellations, which completely remove all seed action contributions generated by the action of a_1 in figure 11.

Cancellation 1 Diagram D.16 exactly cancels the seed action contribution to diagram D.2.

Cancellation 2 Diagram D.18 exactly cancels diagram D.6.

The benefits of the refinements to the diagrammatic procedure are now becoming clear: had we explicitly decorated e.g. diagrams D.6 and D.18 with the external fields, then the single cancellation 2 would be replaced by three separate cancellations; compared to the methodology of [7], we have succeeded in cancelling these terms in parallel.

The gauge remainder of diagrams D.17 and D.19 can be processed using the techniques of section 3.2, to yield the terms of figure 18. The notation

has been adapted since the active field, being an internal field, sits not only on the vertex struck by the gauge remainder but also at the end of a kernel. This kernel attaches to γ and so, rather than using the half-arrow notation of section 3.2, we use the γ to naturally indicate the momentum flow.

$$\begin{aligned}
 & \text{Diagram 1} = \text{Diagram 2} + \text{Diagram 3} \\
 & \text{Diagram 4} = \text{Diagram 5} + \text{Diagram 6}
 \end{aligned}$$

Figure 18: Result of processing the gauge remainders of diagrams D.17 and D.19.

Following section 3.4, we have used charge conjugation to collect terms i.e. the push forward and pull back onto a given field have been combined. In diagram D.23, an additional factor of two arises because the gauge remainder can strike either of the external fields. Note that decoration with the remaining external field now just yields a factor of unity.

Cancellation 3 Diagram D.22 exactly cancels diagram D.20.

Our next task is to examine diagram D.15. Since we are working at $O(p^2)$, and this diagram possesses a structure which is manifestly $O(p^2)$, we expect to be able to directly Taylor expand the rest of the diagram to zeroth order in p . In the case of this particular diagram, this naive expectation is correct. More generally, individual diagrams with an $O(p^2)$ stub may not be Taylor expandable in p ; rather, only sums of diagrams can be Taylor expanded [6, 8], since this procedure can generate IR divergences in individual terms. For reasons that will become apparent, it is actually only worth performing a Taylor expansion in the case that the kernel is decorated (before the Taylor expansion is performed). Diagram D.15 is processed in figure 19.

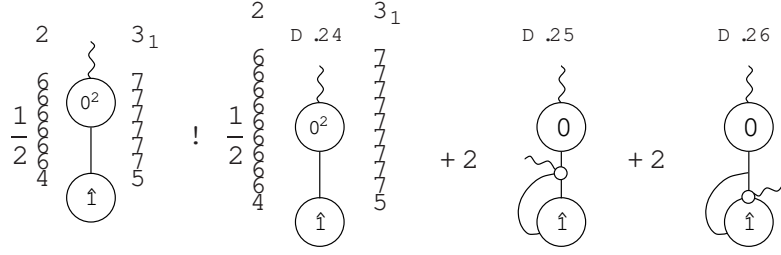


Figure 19: Processing diagram D.15 using the techniques of section 3.3.

There are two things to note. First, in diagrams D.25 and D.26 the top end of the kernel carries zero momentum (at $O(p^2)$) and the bottom end carries the same momentum as the decorative field (not to be confused with the derivative symbol). We have thus combined terms as discussed under equation (5). Secondly, we have not included any diagrams in which the kernel is decorated by the external field and either one loop or no loops. As we know from section 3.4, all such diagrams vanish by charge conjugation invariance, upon recognising that the internal field attached to the two-point, tree level vertex must be an A^1 .

The strategy is now very simple: we iterate the whole procedure. For each of diagrams D.3, D.10 and D.11, we can separate off a manipulable component, which we then convert into a γ -derivative term. Amongst the terms generated will be a dumbbell structure, possessing at least one two-point, tree level vertex. Decorating the two-point, tree level vertices, we can either use the effective propagator relation or we can perform manipulations at $O(p^2)$. There is one subtlety concerning the terms generated when we perform the conversion into γ -derivative terms, which can be illustrated by considering diagram D.11; we isolate the manipulable component in figure 20. In figure 21, we convert diagram D.27 into a γ -derivative term plus corrections.

To proceed, we process both diagrams D.34 and D.35, using the weak coupling flow equations. This is straightforward in the former case and we will not do it explicitly. In the latter case, we must understand how to compute the flow of a reduced, (tree level) vertex. The point is that a reduced vertex lacks a two-point, tree level component, and so the flow of a reduced vertex must lack the flow of a two-point, tree level vertex. From section 3.5.2, we know that the flow of a two-point, tree level vertex generates two two-point, tree level vertices, joined together by an undecorated kernel. Hence, the flow of a reduced tree level vertex must generate a dumbbell structure for which either

at least one vertex is reduced or for which the kernel is decorated. Simplifying the barred notation, where possible, according to (18), we obtain the diagrams of figure 22.

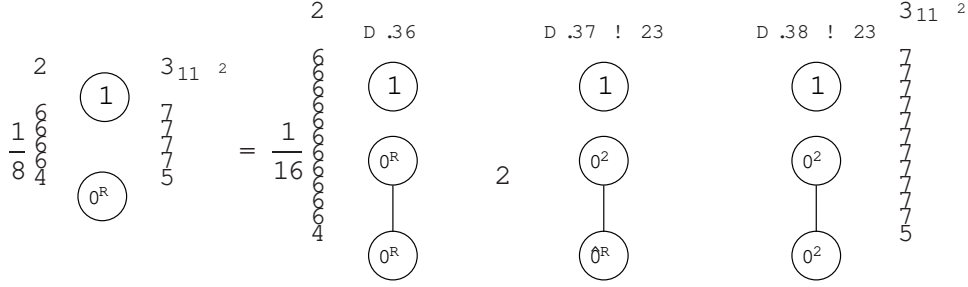


Figure 22: Processing diagrams D.34 and D.35 using the tree-level flow equations.

The next step is the decoration of the two-point, tree level vertices of diagrams D.37 and D.38. Not all of the resultant terms are drawn, but rather the selection shown in figure 23.

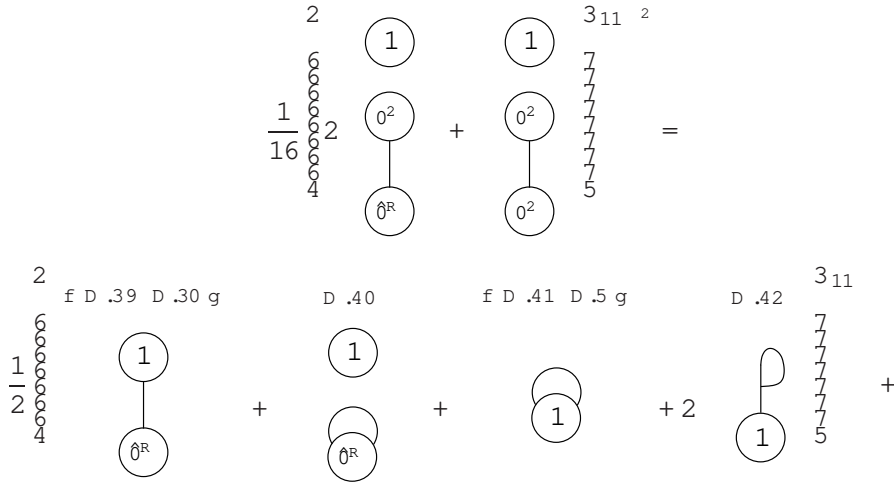


Figure 23: Partial decoration of diagrams D.37 and D.38.

As expected, we find cancellations.

Cancellation 4 Diagram D .39 exactly cancels diagram D .30.

Cancellation 5 Diagram D .41 exactly cancels diagram D .5.

Notice, though, that diagram D .42 does not exactly cancel the Wilsonian effective action component of diagram D 2: to complete the cancellation, we must process diagram D 3. Specifically, we should focus on the $r = 1$ term. A sequence of terms derived from this diagram is shown in figure 24, culminating in the diagram we require to complete the cancellation of the Wilsonian effective action component of diagram D 2.

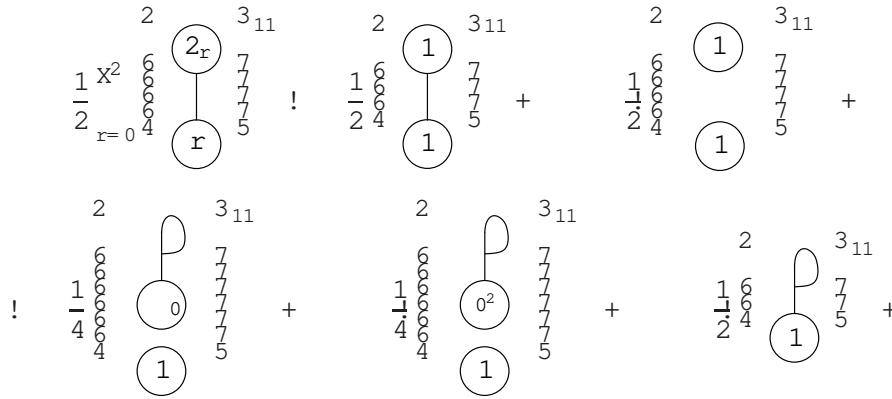


Figure 24: A sequence of terms spawned by diagram D 3.

Iterating the diagrammatic procedure until exhaustion, we find that, up to gauge remainder terms and terms that require manipulation at $O(p^2)$, the calculation reduces to ∂ , ∂^2 , and ∂^3 -derivative terms. The only cancellations involved in this procedure that we have not seen are those which remove terms such as D .31, D .32 and D .40.

The way in which these terms are cancelled is simple. Notice that bottom two structures of the latter two diagrams combine to form a contribution to ∂^2 ; were we to perform the complete diagrammatics, we would find the missing components. The resulting diagram would then cancel against a term spawned from the manipulation of diagram D 3; indeed, this term is included in the ellipsis after the fourth term of figure 24.

We conclude our illustration of the diagrammatic techniques with some further examples of gauge remainders and manipulations at $O(p^2)$. First, consider the diagrams of figure 25.

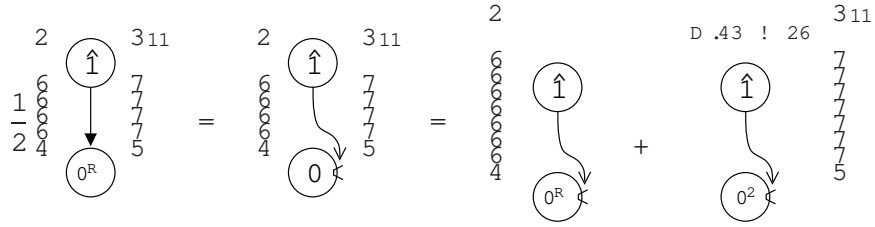


Figure 25: Example of a gauge remainder generated from iterating the diagrammatic procedure.

On the left-hand side, we have a gauge remainder term. On the right-hand side, we have allowed the gauge remainder to act but have not specified which field it strikes, by employing the socket notation of [6]. This socket can be filled by any of the decorations. We have combined the push forward and pullback onto the socket, using charge conjugation invariance, choosing to represent the pair as a pullback (hence the factor of minus two, compared to the parent).

Notice that a gauge remainder striking a reduced vertex generates a full vertex. This is trivial to see: since two-point, tree level vertices are killed by gauge remainders, we can promote a reduced vertex struck by a gauge remainder to a full vertex. Given that the action of the gauge remainder generates a full two-point, tree level vertex, our strategy is as before: we isolate any two-point, tree level contributions and partially decorate them. Amongst the terms generated by this latter procedure are those of figure 26.

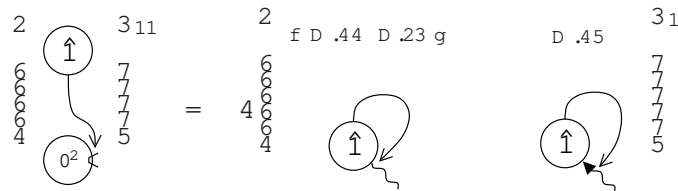


Figure 26: A selection of terms arising from the partial decoration of diagram D.43.

Cancellation 6 Diagram D.44 exactly cancels diagram D.23.

Diagram D.45 is an example of a nested gauge remainder. The action of the nested gauge remainder is exactly the same as for any other gauge

rem ainder. However, we recall from section 3.4 that we cannot generally use charge conjugation invariance to collect together diagrams in which the nested gauge rem ainder has acted.

The next example will demonstrate how diagrams involving processed gauge rem ainders can be converted into γ -derivative terms. Consider the diagrams in figure 27. Notice that the first term is closely related to diagram D.21.

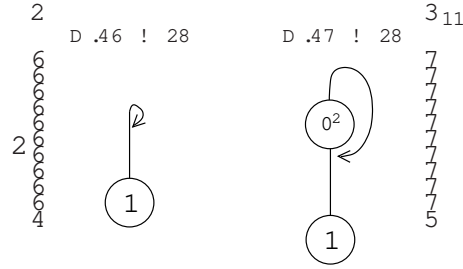


Figure 27: Two diagrams possessing processed gauge rem ainders which can be converted into a γ -derivative term.

Diagram D.47 possesses a structure we have not yet encountered: the two-point, tree level vertex is attached exclusively to internal elds but cannot be removed by the effective propagator relation. Its top socket attaches to a differentiated effective propagator, whereas the attachment of an effective propagator to its bottom socket is interrupted by a processed gauge rem ainder. However, we can make progress by utilising diagrammatic identities (12)–(16) and the tree level flow equation. We have:

$$\begin{aligned}
 & \text{Diagram D.47} = \frac{2}{4} \text{Diagram D.48} - \frac{3}{5} \text{Diagram D.49} \\
 & = \frac{2}{6} \text{Diagram D.50} - \frac{3}{7} \text{Diagram D.51} + \text{Diagram D.52} + \text{Diagram D.53} \\
 & = \text{Diagram D.54}
 \end{aligned} \tag{19}$$

To go from the first line to the second, we have employed diagrammatic identity (15) and the effective propagator relation. On the second line, the first term vanishes courtesy of diagrammatic identity (13); similarly, the second

term, if we employ (16). The final term on the second line vanishes on account of diagrammatic identities (14) and (16):

$$[\gamma] = 0 = \gamma + \gamma = \gamma :$$

It is thus apparent that we can re-write diagrams D.46 and D.47, as shown in figure 28.

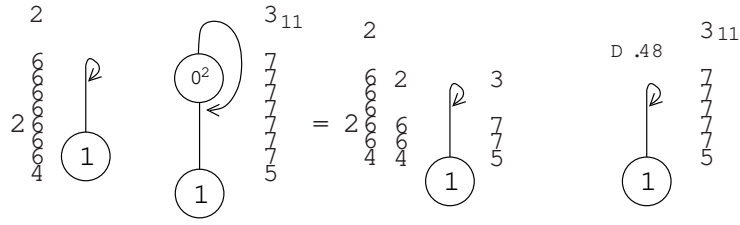


Figure 28: Conversion of diagrams D.46 and D.47 into a -derivative term.

Notice that, amongst the terms generated by processing diagram D.48, is a term which will cancel diagram D.21.

By processing all the gauge remainder terms, we can reduce the calculation to a set of , and -derivative terms, up to those diagrams which require manipulation at $O(p^2)$ and a set of diagrams which do not manifestly cancel. It is easy to find an example of terms of the latter type. When diagram D.21 is cancelled, we know that a gauge remainder term will be left behind, as shown in figure 29.

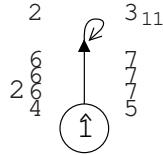


Figure 29: A gauge remainder term which cannot be processed.

The full gauge remainder is trapped, and cannot be processed. The resolution to this problem is trivial, in this case: by charge conjugation invariance, the (necessarily bosonic) kernel has support only in the C^1 and C^2 -sectors;

but these are precisely the sectors where gauge remanders are null. $\triangleleft^2 = 0$ is a (trivial) example of a secondary diagrammatic identity. As we iterate the diagrammatic procedure, we find more complicated examples. The first non-trivial case is [6]



This is one of a family of secondary diagrammatic identities required for the computation of \triangleleft_2 , which are given in [6, 7]. The arbitrary loop generalisation will be presented in [14].

Finally, we will deal with an example involving manipulations at $O(p^2)$, which in turn generate gauge remanders. First, consider the fully decorated diagram on the left-hand side of figure 30, which we manipulate at $O(p^2)$. To get to the second line, we have recognised that

$$\left[\text{Diagram with } 0^2 \text{ and wavy line} \right] = \text{Diagram with } 0^2 \text{ and wavy line} + \text{Diagram with } 0^2 \text{ and wavy line} = \text{Diagram with } 0^2 \text{ and wavy line};$$

as a consequence of the effective propagator relation (where, strictly, this is only true when the structures involved are part of some complete diagram cf. (12)).

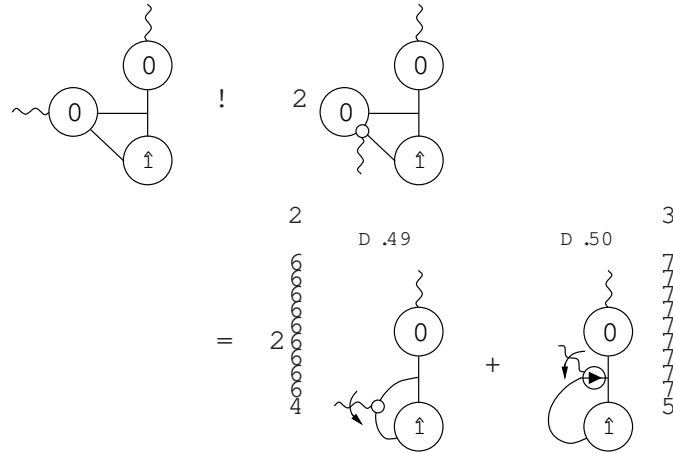


Figure 30: Example of a diagram which can be manipulated at $O(p^2)$.

Diagrams D .25, D .26 and D .49 combine into a total momentum derivative. However, total momentum derivative terms should be discarded, in order that the regularisation scheme be properly defined [4].

With diagram D .50, it looks as though we might be stuck, since the gauge remainder is differentiated with respect to momentum. However, trivially re-drawing

$$\text{Diagram D.50} = \text{Diagram D.51} + \text{Diagram D.52} ;$$

it is clear that progress can be made. In the case that the derivative hits the γ , the γ strikes the kernel and can be processed as usual. In the case that the derivative hits ϕ , we then use diagrammatic identity (15) to yield a striking the one-loop, seed action vertex. We will examine the former case but, rather than dealing directly with diagram D .50, we will deal with the partner diagram (which we will not explicitly generate), coming with opposite sign, in which the one-loop vertex is a Wilsonian effective action vertex, rather than a seed action vertex. We focus on the term in which the gauge remainder pulls back along the kernel. Together with this diagram, we consider two diagrams which can be manipulated at $O(p^2)$, as shown in figure 31.

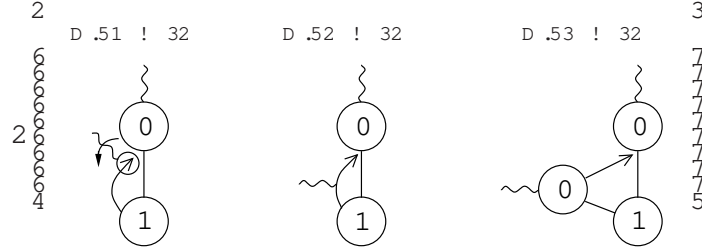


Figure 31: A selection of three terms possessing an $O(p^2)$ stub.

Diagrammatically Taylor expanding the final two terms, we can cast the three diagrams of figure 31 as a ϕ -derivative term. This is most easily seen by noting that

$$\begin{aligned} \text{Diagram D.50} &= \text{Diagram D.51} + \text{Diagram D.52} \\ &= \text{Diagram D.53} + \text{Diagram D.54} : \end{aligned}$$

The first diagram on the second line follows in exactly the same way as (19). The other diagrams on the second line are simply obtained by using the effective

propagator relation. Applying the above relation to diagram D.53 generates several diagrams. The third and fifth die, since they involve a gauge remainder striking a Wilsonian effective action, two-point vertex. The second diagram cancels diagram D.52, after the latter diagram is manipulated at $O(p^2)$. The remaining two diagrams combine with diagram D.51 to form a ∂ -derivative term, as shown in figure 32. Note that, at $O(p^2)$, we can take the ∂_j to strike the entire diagram i.e. including the two-point, tree level vertex decorated by the external field; this follows because the $O(p^2)$ stub is independent of ϕ .

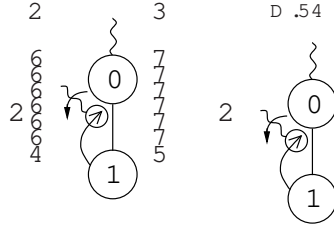


Figure 32: Rewriting diagrams D.51(D.53) as a ∂ -derivative term.

The final points can be made by considering manipulating diagram D.54. We know that the flow of the one-point vertex will generate, amongst other terms, the usual dumbbell structure possessing a two-point, tree level vertex. Applying the effective propagator relation, the Kronecker-terms will cancel diagrams generated elsewhere, leaving behind the trapped gauge remainders shown in figure 33.

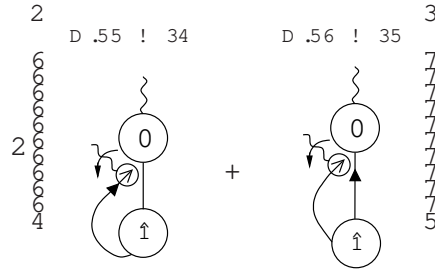


Figure 33: Trapped gauge remainders generated by processing diagram D.54.

Both diagrams D.55 and D.56 can be redrawn. In the former case, we first note from diagrammatic identity (14) that we can move the momentum

derivative from γ to δ , at the expense of a minus sign. Now, since it is true that, in all sectors for which the gauge remainder is not null,

$$\text{Diagram with a circle containing a cross and a wavy line} = \text{Diagram with a circle containing a cross and a wavy line};$$

we can redraw diagram D.55 as shown in figure 34.

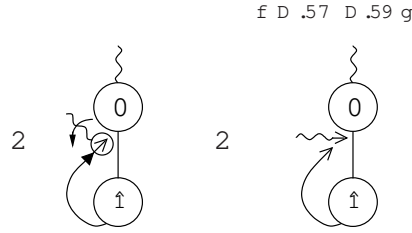


Figure 34: Exact redrawing of diagram D.55.

Diagram D.56 is redrawn, as shown in figure 35.

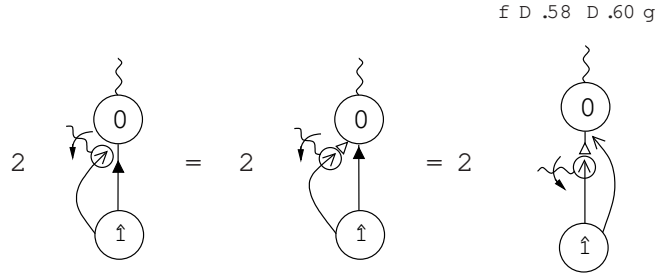


Figure 35: Exact redrawing of diagram D.56.

In the second diagram, if the left-most gauge remainder pushes forward, onto the internal eld, we regenerate the parent. If this gauge remainder pulls back onto the internal eld, the supertrace structure of the diagram is uniquely determined to be $\text{str} A^1 \text{str} A^1 = 0$. If either gauge remainder strikes the external eld, we are left with a two-point, tree level vertex struck by a gauge remainder, which vanishes by diagrammatic identity (13). To go from the second diagram to the third, we allow the right-most gauge remainder to

act; the only surviving contribution is the pull back onto the internal field, giving diagram D .58.

Redrawing diagrams D .55 and D .56 in this manner now allows us to understand how they are cancelled. In figure 36, we show the parent diagram, amongst the daughter diagrams of which, are the terms which yield the cancellations we are looking for.

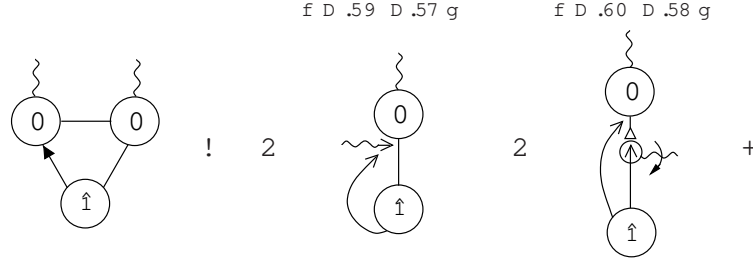


Figure 36: Generation of the diagrams to cancel D .55 and D .56.

Cancellation 7 Diagram D .59 exactly cancels diagram D .57.

Cancellation 8 Diagram D .60 exactly cancels diagram D .58 upon recalling that charge conjugation invariance allows us to reflect a diagram, picking up a sign for each performed gauge remainder and each momentum derivative.

These cancellations could have been performed directly against diagrams D .55 and D .56 by noting that the redrawing of figures 34 and 35 can be thought of as applications of (new) secondary diagrammatic identities. Cancellations 7 and 8 complete the illustration of the \mathcal{D}_2 diagrammatics; the diagrammatic procedure is summarised in the flow chart of figure 37.

Iterating the entire procedure until exhaustion, we can reduce the calculation to a set of \mathcal{D}_1 and \mathcal{D}_0 -derivative terms and a set of $\mathcal{O}(p^4)$ terms'. Diagram D .24 is an example of a term of the latter type; it can be easily demonstrated, using the Ward identities, that the sum of these terms vanish at $\mathcal{O}(p^2)$ [6,7]. The \mathcal{D}_0 -derivative and \mathcal{D}_1 -terms can be simplified by utilising the diagrammatic expression for \mathcal{D}_1 [6,8], to yield an expression for \mathcal{D}_2 in terms of just \mathcal{D}_0 and \mathcal{D}_1 -derivative terms. As mentioned already, the \mathcal{D}_0 -terms vanish in the limit that $\epsilon \rightarrow 0$. It is beyond the scope of this paper to describe the extraction of the numerical coefficient from the final set of terms; these techniques are fully described in [6,8] (see also [13] for an example of their application in a simplified context).

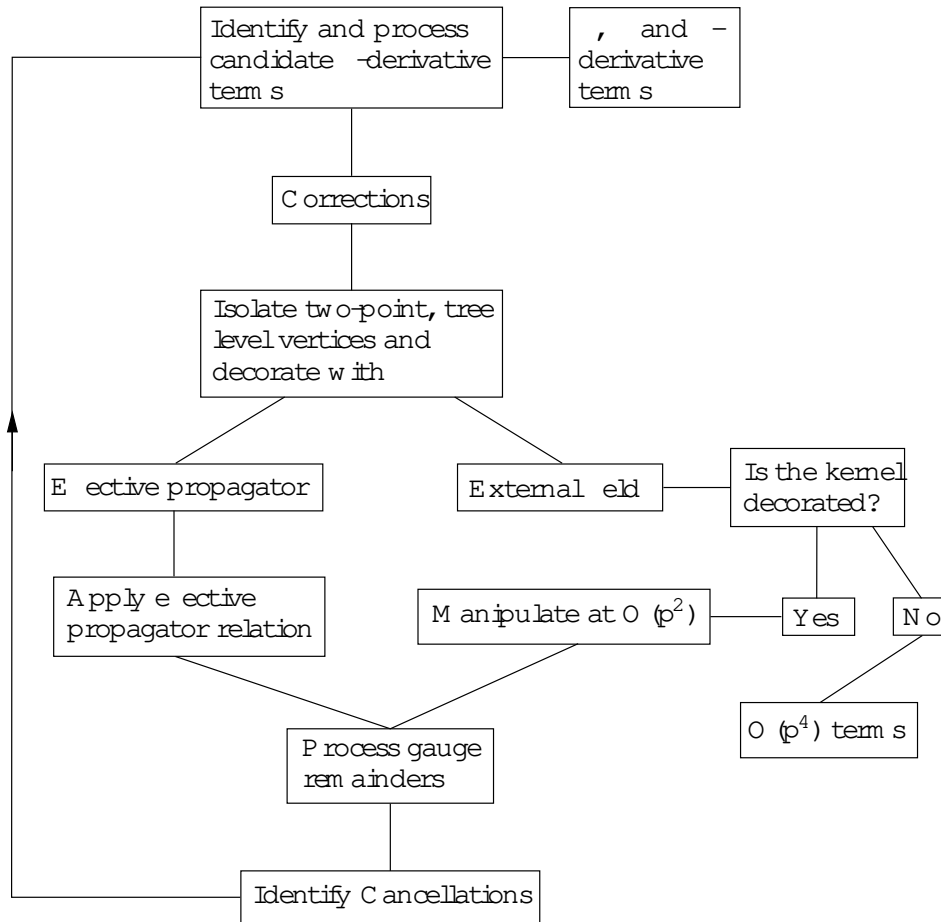


Figure 37: The diagrammatic procedure.

Acknowledgements I acknowledge financial support from PPARC Rolling Grant PPA/G/O/2002/0468.

References

- [1] T.R.Morris, Nucl.Phys.B 573 (2000) 97, [arXiv:hep-th/9910058].
- [2] T.R.Morris, JHEP 0012 (2000) 012, [arXiv:hep-th/0006064].
- [3] S.Amone, A.Gatti and T.R.Morris, Phys. Rev. D 67 (2003) 085003, [arXiv:hep-th/0209162].

- [4] S. Amone, Y. A. Kubyshin and T. R. Morris, J. F. Tighe, Int. J. Mod. Phys. A 17 (2002) 2283, [[arXiv:hep-th/0106258](#)].
- [5] O. J. Rosten, T. R. Morris and S. Amone, The Gauge Invariant ERG, Proceedings of Quarks 2004, Pushkinskie Gory, Russia, 24-30 May 2004, <http://quarks.inrac.ru>, [[arXiv:hep-th/0409042](#)].
- [6] O. J. Rosten, The Manifestly Gauge Invariant Exact Renormalisation Group', Ph.D. Thesis, [[arXiv:hep-th/0506162](#)].
- [7] S. Amone, T. R. Morris and O. J. Rosten, [[arXiv:hep-th/0507154](#)].
- [8] T. R. Morris and O. J. Rosten, A Manifestly Gauge Invariant, Continuum Calculation of the $SU(N)$ Yang-Mills two-loop β function', SHEP 05-22.
- [9] Work in progress.
- [10] J. I. Latorre and T. R. Morris, JHEP 0011 (2000) 004, [[arXiv:hep-th/0008123](#)]; J. I. Latorre and T. R. Morris, Int. J. Mod. Phys. A 16 (2001) 2071, [[arXiv:hep-th/0102037](#)].
- [11] S. Amone, A. Gatti and T. R. Morris JHEP 0205 (2002) 059, [[arXiv:hep-th/0201237](#)].
- [12] S. Amone, A. Gatti, T. R. Morris and O. J. Rosten, Phys. Rev. D 69 (2004) 065009, [[arXiv:hep-th/0309242](#)].
- [13] S. Amone, T. R. Morris and O. J. Rosten, [[arXiv:hep-th/0505169](#)].
- [14] O. J. Rosten, In preparation.
- [15] I. Bars, in Introduction to Supersymmetry in Particle and Nuclear Physics, eds. Castanes et al. (Plenum, New York, 1984) 107.
- [16] T. R. Morris, in: The Exact Renormalization Group, Eds. K. Raznits et al. (World Sci, Singapore, 1999) p.1, [[arXiv:hep-th/9810104](#)].
- [17] T. R. Morris, Prog. Theor. Phys. Suppl. 131 (1998) 395, [[arXiv:hep-th/9802039](#)].